Low-cost micron-sized silicon/carbon anode prepared by a facile ball-milling method for Li-ion batteries

Yueqiang Lin, Bin Qi, Zhiyuan Li, Su Zhang*, Tong Wei, Zhuangjun Fan*

School of Material Science and Engineering, China University of Petroleum, Qingdao, 266580, China

*Corresponding authors: suzhangs@163.com (S. Zhang); fanzhj666@163.com (Z. Fan)

Abstract. Commercially, Si nanoparticles (nano Si) are blended with graphite to construct high-capacity Si/C anodes. However, this strategy falls short because of the high cost of nano Si, serious pollution due to the use of organic solvent, and weak physical-electrical connection between graphite and Si. Herein, using low-cost micron-sized Si (μ Si) and graphite as the raw materials, we proposed a facial ball-milling method to construct high-performance Si/C anode (μ Si/C@CH) in which milled Si particles are protected both by graphite matrix and homogeneous chitosan-derived carbon layer. It is shown that the N and O atoms not only tend to coordinate with Li+, generating uniformly-distributed Li+ transport channels, but also improve the electrical conductivity of the anode materials. As a result, μ Si/C@CH shows high cycling stability (376.7 mAh g-1 at 0.5 A g-1 after 500 cycles) and good rate capability of 120.2 mAh g-1 at 5 A g-1. This dual protection strategy facilitates the practical application of Si/C materials in high-energy density Li ion batteries (LIBs).

Keywords: μSi/C; LIBs; chitosan; high stability; interface modification.

1. Introduction

Si with a high theoretical specific capacity of 3580 mAh g-1 (Li15Si4) and a low lithiation potential (~0.3 V vs. Li+/Li) is regarded as promising anode materials for high-energy density Li ion batteries (LIBs) [1]. However, the large volume change of ~300 during the lithiation/delithiation process and poor conductivity of Si restrict its practical application seriously. Commercially, Si are combined with graphite to construct Si/C anode materials, in which graphite with good conductivity and mechanical ductility serves as the buffer matrix [2]. However, current research on the preparation of Si/C materials is usually carried out by physically mixing nano Si and graphite in organic solvent, which is not only hard to uniformly distribute Si in the graphite matrix, but also leads to serious pollution and high cost [3, 4]. Moreover, Si particles are usually randomly distributed on the surface of graphite with weak interfacial interaction, which makes it easily detach from the graphite conductive network during the lithiation/delithiation process. Additionally, the direct exposure of Si interface to the electrolyte results in unstable solid electrolyte interface (SEI), which can fully insulate the electrons after it grows thicker.

Chitosan is a cheap and environment friendly polymer consisted of glucosamine unites. The O and N atoms in glucosamine can serve as lithiophilic sites [1], promoting Li+ transport in the anodes. Herein, with the assistance of chitosan, we proposed a facial ball-milling method to construct high-performance Si/C anode (μSi/C@CH). On one hand, the chitosan-derived carbon layer separates μSi/C from the electrolyte, suppressing side reactions. On the other hand, N, O atoms not only improve Li+ transport but also improve the electrical conductivity of Si/C materials significantly. Benefiting from the above merits, the cycle stability and rate performance of μSi/C@CH are significantly superior to μSi/C and graphite anodes. After 500 cycles at 0.5 A g-1, a high reversible capacity of 376.7 mAh g-1 was maintained. Even at 5 A g-1, the capacity of μSi/C@CH anode still reaches 120.2 mAh g-1, 2.4 times higher than that of μSi/C anode (49.7 mAh g-1). Our method is straightforward, cost-effective, and eco-friendly, promoting the practical application of Si/C materials.

2. Experimental

2.1 Materials

Graphite and chitosan were purchased from Shanghai Aladdin Co., Ltd. μSi with an average diameter of 5 μm was purchased from Shanghai ST-Nano Science & Technology Co., Ltd. All the materials and reagent are analytical grade and used without further purification.

2.2 The synthesis of μSi/C and μSi/C@CH

Ball-milling was used to prepare μSi/C and μSi/C@CH. Certain amount of graphite powder, μSi, and chitosan were blended in a zirconia jar with a ball-to-powder weight ratio of 10:1. The ball-milling process was carried out at 500 r min-1 in air atmosphere. The final product was denoted as μSi/C@CH. Similarly, μSi/C was synthesized following the same procedure without the introduction of chitosan.

2.3 Characterization

The morphology and structure of the as-prepared samples were measured by scanning electron microscopy (SEM, SU70-HSD), X-ray powder diffraction (XRD), Raman microscope (laser wavelength of 514.5 nm), and N2 adsorption/desorption at 77 K (Quantachrome NOVA 2000 surface analyzer). The conductivity was carried out using a four-point probe conductivity testing equipment.

2.4 Electrochemical Measurement

The electrode slurry was prepared by mixing 80 wt.% of the active material, 10 wt.% of carbon black and 10 wt.% of sodium-alginate binder in proper amount of deionized water. The prepared slurry was casted onto a 10 μm thick copper foil and then dried at 80 ℃ for 12 h.

All cells were tested between 0.01−1.0 V (vs. Li/Li+) by a LAND CT2001A system (all half cells were activated at a small current density of 0.05 A g-1 for three cycles). Cyclic voltammetry (CV) was carried out in the potential range of 0.01−1.0 V (vs. Li/Li+) at scanning rates of 0.05 mV on the Solartron Modulab. Electrochemical impedance spectroscopy (EIS) measurements were conducted on the Solartron Modulab in the frequency range from 100 kHz to 0.01 Hz with a voltage amplitude of 10 mV. The EIS curves of the electrodes were fitted by a modified Randles-Ershler equivalent circuit [5], where the charge transfer resistance (Rct) at the electrolyte/electrode interface corresponds to the semicircle at the medium region. And the Li+ diffusion effiencient (DLi+) was calculated according to the following formula [5-7].

$$Z^{'} = R_S + R_{ct} + \sigma\omega^{-1/2}$$

$$D_{Li}^{+} = \frac{R^2T^2}{2A^2n^4F^4C_{Li}^2\sigma^2}$$

3. Results and discussion

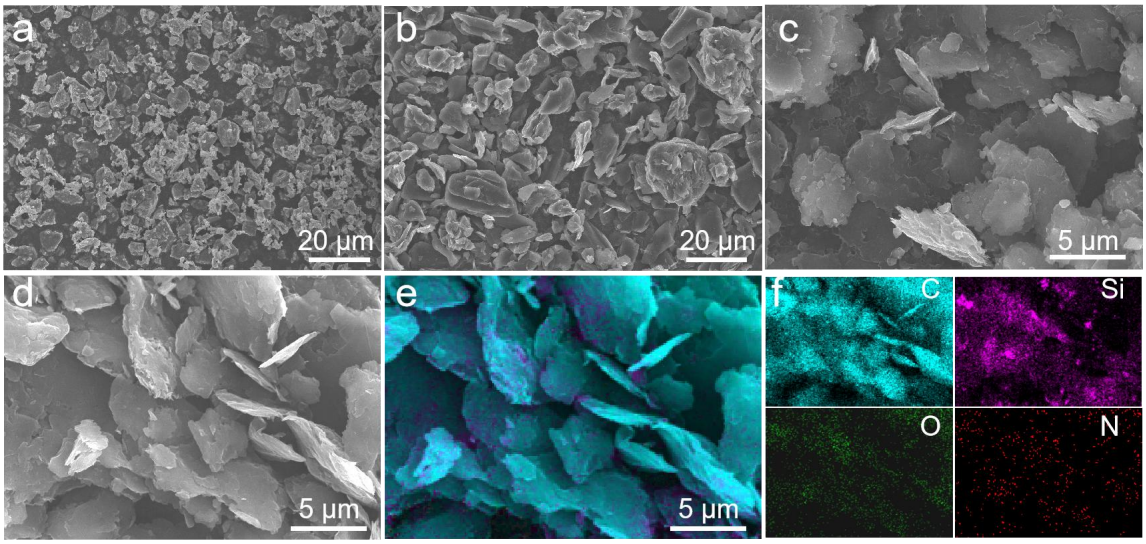

Fig. 1. SEM images of (a) μSi, (b) commercial graphite, (c) μSi/C, (d) μSi/C@CH, and (e-f) EDS elemental mapping analysis of μSi/C@CH.

The particle size of the μSi used in this work ranges from 1 μm to 10 μm (Fig. 1a). Commercial graphite has a smooth surface with a particle size of 5-20 μm (Fig. 1b). After the ball-milling treatment, both the particle sizes of μSi/C (Fig. 1c) and μSi/C@CH (Fig. 1d) are decreased to ~5 μm, indicating the addition of chitosan has little influence on the size of the ball-milled particles. However, compared with μSi/C, the surface of μSi/C@CH is more smooth, which is due to the protection of chitosan layer in the ball-milling process. Furthermore, EDS elemental mapping (Fig. 1e-f) shows O and N which originate from chitosan are uniformly distributed, suggesting continuous and homogeneous chitosan coating is formed on the surface of μSi/C@CH.

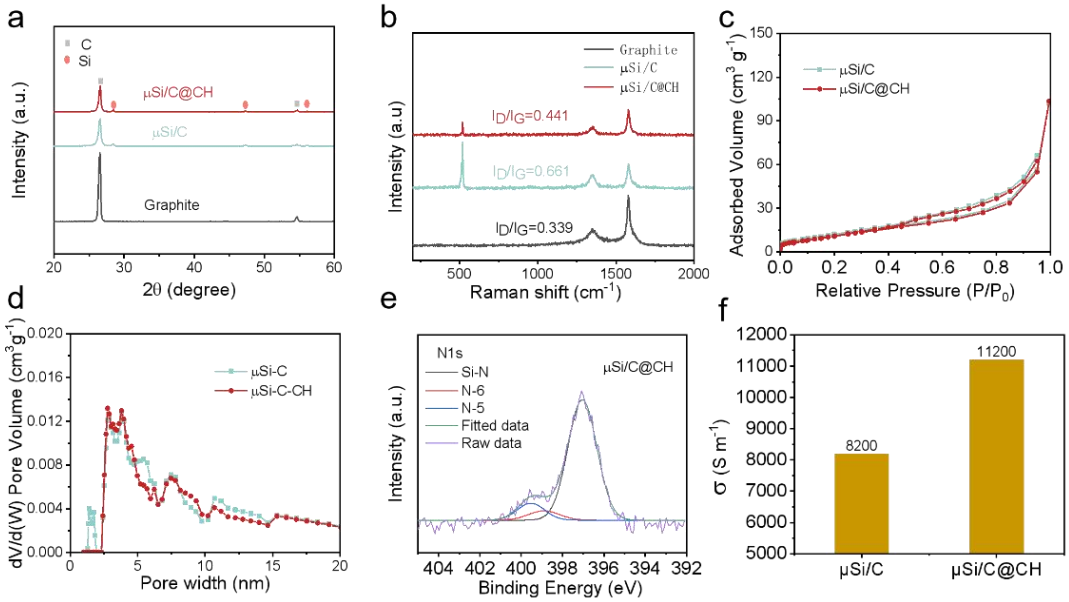

Fig. 2. (a) XRD and (b) Raman spectra of graphite, μSi/C, and μSi/C@CH. (c) N_2 adsorption-desorption isotherms and (d) the pore size distribution of μSi/C and μSi/C@CH. (e) High-resolution N 1s XPS spectrum of μSi/C@CH. (f) The electrical conductivity comparison of μSi/C and μSi/C@CH.

Fig. 2a exhibits the XRD spectra of graphite, μSi/C, and μSi/C@CH. The peaks at approximately 22° and 54° are attributed to graphite, and diffraction peaks at 28.4°,

47.6 ° , and 56.2 ° correspond to lattice planes of crystal Si, respectively. The diffraction peaks of Si fit well with those of crystal Si (JCPDF No. 27-1402) [8], meaning the crystal structure of Si is not destroyed in the ball-milling process. Compared with μ Si/C, the intensity of XRD peaks for μ Si/C@CH is weaker, which is due to the encapsulation of μ Si/C by chitosan-derived carbon layer. Chitosan encapsulation is also confirmed by a weak Si peak at 510 cm-1 in the Raman spectra (Fig. 2b). Additionally, the D peak at ~1380 cm-1 is generally considered to represent the structure disorder in carbon materials, while G peak at around 1580 cm-1 refers to the in-plane E2g bond-stretching motion of graphitic lattice (sp2 carbon) [9]. Their intensity ratio (ID/IG) is usually adopted to represent the internal defects of carbon materials. The ID/IG of μ Si/C and μ Si/C@CH are 0.661 and 0.441, respectively, significantly higher than that of graphite (0.339) without ball-milling, indicating that the ball-milling process introduced defects in graphite. However, ID/IG of μ Si/C@CH is smaller than that of μ Si/C, which is due to the protection of chitosan. It is commonly believed that defects including holes and edges tend to induce severe side reaction with the electrolytes. Therefore, a lower ID/IG ratio of μ Si/C@CH is expected to contribute a higher initial coulombic efficiency and thus better cycle performances [10]. The protection of chitosan was also evidenced by a slightly lower specific surface area of 45.89 m2 g-1 for μ Si/C@CH than that of 47.65 m2 g-1 for μ Si/C (Fig. 2c-d).

XPS analysis indicates a strong Si-N bond appears in μ Si/C@CH (Fig. 2e), which is formed with the assistance of high-energy ball-milling. The Si-N bond not only enhances the interfacial interaction between Si and chitosan-derived carbon layer, but also improves the conductivity of μ Si/C@CH [11]. As proved by the conductivity test (Fig. 2f), the electrical conductivity of μ Si/C@CH reaches 11200 S m-1, superior to that of μ Si/C (8200 S m-1).

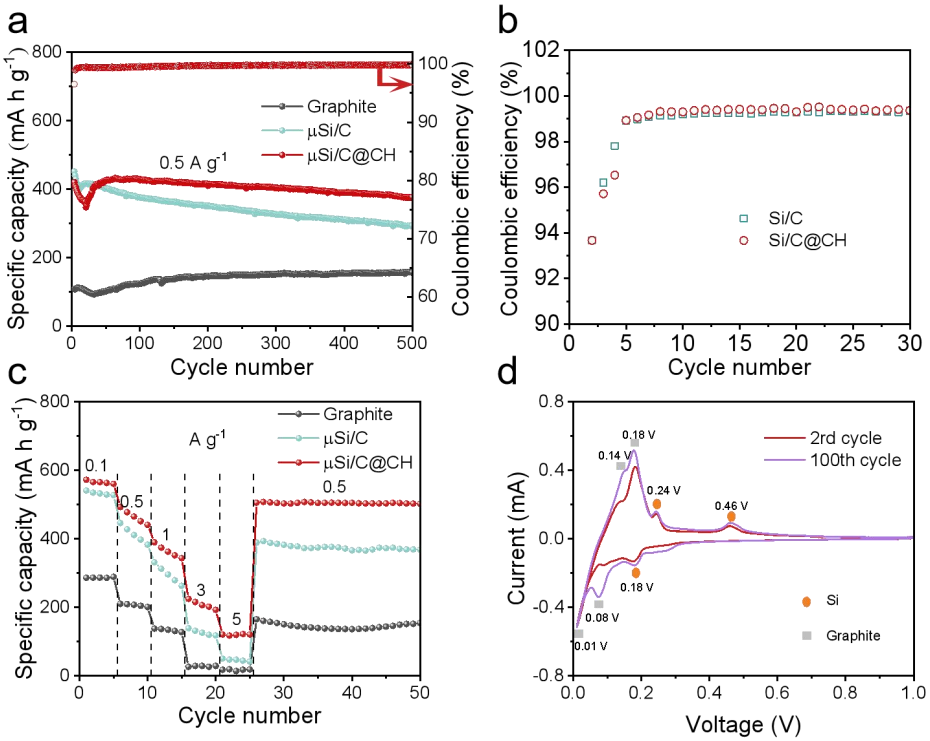

Fig.3. (a) Cycling stability, (b) Coulombic efficiency (CE) changes, (c) rate capability of graphite, μSi/C, and μSi/C@CH anodes. (d) The CV curves of μSi/C@CH electrode at different cycle numbers for a scan rate of 0.05 mV s^{-1}.

The homogenous chitosan coating with abundant N, O atoms ensures good electrochemical performance of μ Si/C@CH anode. Si/C@CH electrode achieved a high reversible capacity retention of 89.4% (376.7 mAh g-1) at 0.5 A g-1 after 500 cycles, significantly higher than 64.7% of Si/C electrode (Fig.3a). Moreover, μ Si/C@CH electrode reached a Coulombic efficiency (CE)

above 99% in the 5th cycle and maintained a higher CE than μ Si/C electrode in the following cycles (Fig.3b). Homogeneously-coated chitosan-derived carbon layer prevents direct exposure of μ Si/C surface to the electrolyte, suppressing side reactions and thus leading to a stable SEI for μ Si/C@CH electrode [12]. Additionally, benefiting from the high conductivity of μ Si/C@CH, good rate performance of 120.2 mAh g-1 at 5 A g-1 is obtained for μ Si/C@CH electrode (Fig.3c). No obvious peak shift was observed for the CV curve of μ Si/C@CH electrode at the 100th cycle compared with the 2nd cycle (Fig.3d), further confirming its highly stable electrochemical performance [13].

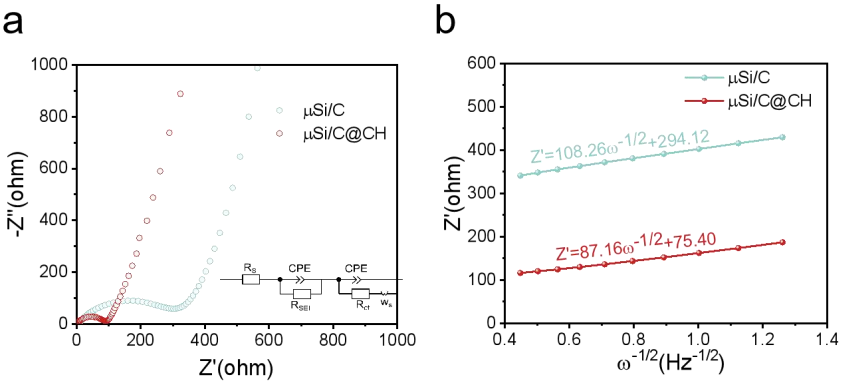

Fig. 4. (a) Nyquist plots and (b) linear fitting of Z' versus $\omega^{-1/2}$ relationship of μSi/C and μSi/C@CH electrodes.

The enhanced Li+ transport through chitosan coating is reflected by a smaller charge transfer resistance (Rct) of 33.9 Ω for μ Si/C@CH electrodes, compared with 143.6 Ω for μ Si/C electrode (Fig. 4a). In addition, the calculated Li+ diffusion coefficient (DLi+) of μ Si/C@CH electrode is 9.31×10-13 cm2 s-1, higher than that of μ Si/C electrode (6.03×10-13 cm2 s-1). This indicates the chitosan coating facilitates e-/Li+ transport by providing uniform e-/Li+ pathways.

4. Summary

In summary, we proposed a facile ball-milling method to prepare high-performance Si/C anodes. The milled Si particles are protected both by graphite matrix and homogeneous chitosan-derived carbon layer. The homogeneous chitosan coating with abundant N , O atoms not only serves as the protective shell but also are supposed to coordinate with Li+, promoting Li+ transport. Therefore, μ Si/C@CH electrode displays a high capacity retention of 89.4% at 0.5 A g-1 after 500 cycles. Even at 5 A g-1, the capacity still reaches 120.2 mAh g-1. This strategy is straightforward, cost-effective, and eco-friendly, providing solutions for constructing high-energy density LIBs.

References

[1] L. Li, C. Fang, W. Wei, L. Zhang, Z. Ye, G. He, Y. Huang, Nano-ordered structure regulation in delithiated Si anode triggered by homogeneous and stable Li-ion diffusion at the interface, Nano Energy, 72 (2020) 104651.

[2] X. Xue, X. Liu, B. Lou, Y. Yang, N. Shi, F. Wen, X. Yang, D. Liu, The mitigation of pitch-derived carbon with different structures on the volume expansion of silicon in Si/C composite anode, J. Energy Chem., 84 (2023) 292-302.

[3] L. Sun, Y. Liu, J. Wu, R. Shao, R. Jiang, Z. Tie, Z. Jin, A Review on Recent Advances for Boosting Initial Coulombic Efficiency of Silicon Anodic Lithium Ion batteries, Small, 18 (2022) 2102894.

[4] N. Kim, Y. Kim, J. Sung, J. Cho, Issues impeding the commercialization of laboratory innovations for energy-dense Si-containing lithium-ion batteries, Nat. Energy, 8 (2023) 921-933.

[5] W.U. YongJian, T. RenHeng, L.I. WenChao, W. Ying, H. Ling, O. LiuZhang, A high-quality aqueous graphene conductive slurry applied in anode of lithium-ion batteries, J. Alloy Compd., 830 (2020) 154575.

[6] W. Xu, K. Zhao, C. Niu, L. Zhang, Z. Cai, C. Han, L. He, T. Shen, M. Yan, L. Qu, L. Mai, Heterogeneous branched core–shell SnO2–PANI nanorod arrays with mechanical integrity and three dimentional electron transport for lithium batteries, Nano Energy, 8 (2014) 196-204.

[7] N. Ding, J. Xu, Y.X. Yao, G. Wegner, X. Fang, C.H. Chen, I. Lieberwirth, Determination of the diffusion coefficient of lithium ions in nano-Si, Solid State Ionics, 180 (2009) 222-225.

[8] Y. Zhang, R. Zhang, S. Chen, H. Gao, M. Li, X. Song, H.L. Xin, Z. Chen, Diatomite-Derived Hierarchical Porous Crystalline-AmorphousNetwork for High-Performance and Sustainable Si Anodes, Adv. Funct. Mater., 30 (2020) 2005956.

[9] N. Cheng, J. Pan, M. Shi, Q. Hou, Y. Han, Using Raman spectroscopy to evaluate coal maturity: The problem, Fuel, 312 (2022) 122811.

[10] L. Han, X. Zhu, F. Yang, Q. Liu, X. Jia, Eco-conversion of coal into a nonporous graphite for high-performance anodes of lithium-ion batteries, Powder Technol., 382 (2021) 40-47.

[11] A. Hendaoui, A. Alshammari, Preparation of Nitrogen-doped Holey Multilayer Graphene Using High-Energy Ball Milling of Graphite in Presence of Melamine, Materials 2023, 16, 219.

[12] S. Pan, J. Han, Y. Wang, Z. Li, F. Chen, Y. Guo, Z. Han, K. Xiao, Z. Yu, M. Yu, S. Wu, D.-W. Wang, Q.-H. Yang, Integrating SEI into Layered Conductive Polymer Coatings for Ultrastable Silicon Anodes, Adv. Mater., 34 (2022) 2203617.

[13] F. Zhang, H. Xia, T. Wei, H. Li, M. Yang, A.-M. Cao, A New Universal Aqueous Conductive Binder via Esterification Reinforced Electrostatic/H-bonded Self-assembly for High Areal Capacity and Stable Lithium-Ion Batteries, Energy Environ. Sci., (2023).